World Academy of Science, Engineering and Technology
International Journal of Electronics and Communication Engineering
Vol:9, No:2, 2015

# Numerical Simulation of Thermo-Fluid Behavior in Wavy Microchannel Used in Microelectronic Devices

A. Balabel, A. F. Khadrawi, Ali S. Al-Osaimy



***Abstract*****—**The hydrodynamic and thermal behaviors of fluid flow in wavy microchannel are investigated numerically. Effects of Reynolds number on the hydrodynamics and thermal behaviors are investigated. Three cases of Reynolds number (580, 1244, and 1910) are adopted in this study. It is found that the separation zone begin appears when Reynolds number is greater than 1910 at the end-section of the wave. Also it is found that dimensionless maximum velocity at the mid-section of the wave decreases and becomes as a turbulent behavior as Reynolds numbers increases. The maximum temperature at the center line at the mid-section of the wave increases as Reynolds number increases until it reaches the turbulent behavior when Reynolds number is equal or greater than 1244, while this behavior will be achieved at very high velocities at the end section of the wave.

***Keywords*****—**Thermo-Fluid Behavior, Microelectronic Devices, Numerical Simulation, Wavy Microchannel.

## I. Introduction

DUE to fast increase in power density and reduction of electronic packages, traditional cooling techniques using fans or metal fins may be unpractical or unable to meet the quick increasing cooling demands of emerging electronic devices. The thermal issue is now a critical neck for further improvement of advanced electronic devices. If no work is taken to improve more effective and innovative cooling technique, reduced in mean-time-to-failure and performance retraction will culminated. One favorable solution to the problem is direct liquid cooling merging microchannels [1]–[7]. Pertinent studies involve single- phase cooling and two-phase cooling. While another has a potentially higher heat removal capacity, it includes complex issues such as condensation, saturation temperature, critical heat flux, nucleation site etc. For average heat fluxes, single-phase cooling suggests an alternative that is simpler to accomplish and is thus preferable [4]. Regarding to single-phase cooling, due to the reduced feature size of microchannels and the increased effect of surface tension, high flow rates will cause a sever increase in pressure loss and hence pumping power.

Recently, fully developed laminar flow and heat transfer in periodic serpentine channels with various cross-section shapes is investigated numerically [8]-[12]. It is found that Dean Vortices and more complex vertical flow patterns emanate when the coolant of liquid is flowing through the bends. The heat transfer performance was greatly improved through straight channels with the same cross section; at the same time the pressure drop gruel is much smaller than the heat transfer enhancement. Laminar force convection in wavy plate fin channels under periodically developed air flow condition is investigated numerically [13], [14]. Their two-dimensional simulation proved that the flow was characterized by lateral swirl or fluid recirculation in the tub regions of the wavy channel; the three-dimensional simulation detected symmetric Dean vortex pairs in the cross sections of the sinusoidal channels. There are many several interests in research interest of micro-devices over the last years [15]-[20]. All these researches were in conventionally straight microchannels.

In the present work thermal and hydrodynamic behaviors of fluid flow in wavy microchannel are investigated numerically. Effect of different cases of Reynolds number is investigated in this study. The thermal and hydrodynamics behaviors are investigated under these cases. The numerical procedure developed in this work is based on the control volume approach proposed by Patankar [21].

## II. Material and Methods

In microchannel environment, shown in Fig. 1, the thermally laminar flow is governed by the continuity, momentum and energy equations for unsteady, incompressible and Newtonian flow. Regarding above assumptions, the governing equations are written as:

$$\nabla \cdot (\rho u) = 0 \tag{1}$$

$$\frac{\partial(\rho u)}{\partial t} + \nabla \cdot (\rho u u) + \nabla p = \nabla \cdot (2\mu S) \tag{2}$$

$$\frac{\partial(\rho T)}{\partial t} + \nabla \cdot (\rho u T) = \nabla \cdot (q / C_p) \tag{3}$$

The strain rate tensor components can be described as:

$$S_{ij} = 0.5(\frac{\partial u_i}{\partial x_j} + \frac{\partial u_j}{\partial x_i}) \tag{4}$$

and,

$$q = -C_p(\frac{\mu}{\Pr})\nabla T \tag{5}$$

A. Balabel, A. F. Khadrawi, and Ali S. Al-Osaimy are with the CFD-Lab, Mechanical Engineering Dept., Faculty of Engineering, Taif University, Al-Haweiah, P.O. 888, Z.C. 21974, Taif, Saudi Arabia (e-mail: ashrafbalabel@yahoo.com, khadrawi99@yahoo.com, alosaimy@tu.edu.sa).

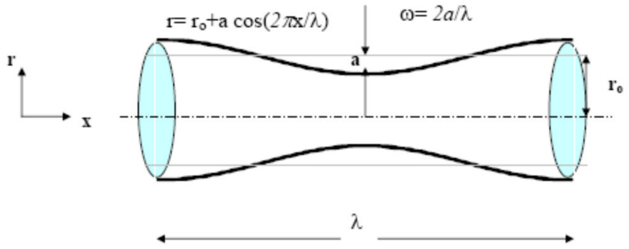


Fig. 1 Configuration of wavy microchannel

The molecular Prandtl number *Pr* and the specific heat capacity at constant pressure are defined according to the fluid considered. The numerical procedure developed in the present work is based on the control volume approach proposed by [21]. In such approach, a general differential equation for the dependent variables ($u$, $v$, $T$) is written for unsteady, Newtonian, two-dimensional and incompressible flow as:

$$\frac{\partial}{\partial t}(\rho\varphi)+\frac{\partial}{\partial x}(\rho u\varphi)+\frac{\partial}{\partial y}(\rho v\varphi)=\frac{\partial}{\partial x}(\Gamma_{\varphi}\frac{\partial\varphi}{\partial x})+\frac{\partial}{\partial y}(\Gamma_{\varphi}\frac{\partial\varphi}{\partial r})+S_{\varphi} \quad (6)$$

The quantities $\Gamma_{\varphi}$ and $S_{\varphi}$ are specific to a particular meaning of $\varphi$ .Using the control volume arrangement proposed by [21], the above general differential equation can be written in terms of the total fluxes over the control volume faces and the resulting equation is integrated over each control volume. In similar manner, the continuity equation is integrated over the control volume.

In our algorithm, one can assume that the velocity field reaches its final value in two stages; that means

$$\mathbf{u}^{n+1}=\mathbf{u}^{*}+\mathbf{u}_{c} \quad (7)$$

where by, $\mathbf{u}^{*}$ is an imperfect velocity field based on a guessed pressure field, and $\mathbf{u}_{c}$ is the corresponding velocity correction. Firstly, the 'starred' velocity will result from the solution of the momentum equations. The second stage is the solution of *Poisson* equation for the pressure

$$\nabla^{2}p_{c}=\frac{\rho}{\Delta t}\nabla\cdot\mathbf{u}^{*} \quad (8)$$

where $p_{c}$ will be called the pressure correction and $\Delta t$ is the chosen time step. Once this equation is solved, one gets the appropriate pressure correction, and consequently, the velocity correction is obtained according to:

$$\mathbf{u}_{c}=-\frac{\Delta t}{\rho}\nabla p_{c} \quad (9)$$

The fractional step non-iterative method described above ensures the proper velocity-pressure coupling for incompressible flow field. It should be pointed out that the above numerical method has been developed and successfully applied for simulating a variety of engineering applications [22]-[25]. In order to accurately calculate the surface force that included in the momentum equations a simple linear interpolation is used firstly to calculate any property of the interface from the known internal grid point's values. According to Fig. 2, the Poisson equation for pressure is approximated at point **p** as:

$$p_{ij}=\left[\frac{p_{a}}{h_{a}(h_{a}+h_{b})}+\frac{p_{b}}{h_{b}(h_{a}+h_{b})}+\frac{p_{c}}{h_{c}(h_{c}+h_{d})}+\frac{p_{c}}{h_{d}(h_{c}+h_{d})}+S_{p}\right] \quad (10)$$

where $S_p$ is the source term described in (8).

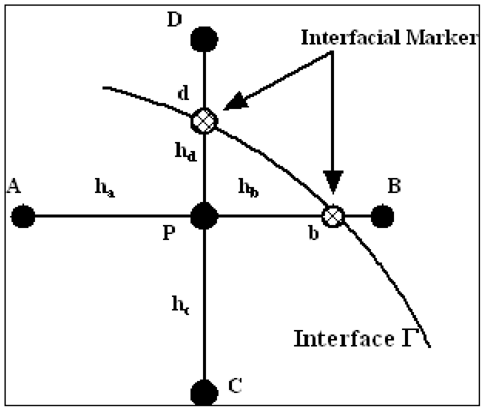


Fig. 2 Calculation of the interphase boundary values

## III. Results and Discussion

Numerical simulation of fluid behavior in wavy microchannel used in microelectronic devices is investigated in this study. Axial velocity distribution and the velocity vector plot for case I, case II, and case III are shown in Figs. 3 and 4. Fig. 3 shows that the centerline velocity increases as the Reynolds number increases for the same wave ratio. The increase is due to the satisfying of the continuity equation; especially at the midsection of the wave. Fig. 4 indicates the same behavior for the axial velocity distribution in form of vector plots. Fig. 5 shows the dimensionless velocity profiles at the mid-section of the wave for the different cases considered. It is clear that the dimensionless maximum velocity at the center line at the mid-section of the wave (throttling-section) increasing with decreasing Reynolds number at the inlet. This is due to as increasing Reynolds number at the inlet, the velocity at the center line will increase greatly due throttling and the flow behavior will approach the turbulent behavior and it becomes as a vertical straight line with decreasing in the boundary layer in order to satisfy the continuity equation, while this is not correct at the end-section of the wave because there is no throttling and the turbulent behavior may occurs at very high velocities as shown in Fig. 6. The existence of flow separation at the end-section of the wave for the different cases considered is shown in Fig. 7. It is clear that the flow separation may occur at high velocities (Re > 1910).

Figs. 8 and 9 show the temperature profiles at the mid and end sections of the wave for the different cases considered. It is obvious from these figures that the turbulent behavior will be achieved at the mid-section at Re > 1244, also, the thermal boundary layer decreases as the inlet velocity increases as shown in Fig. 8. While the thermal turbulent behavior at the end-section of the wave will be achieved at very high velocities (Re >1900) as shown in Fig. 9.

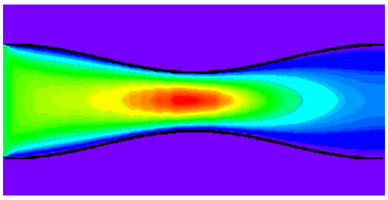

(a)

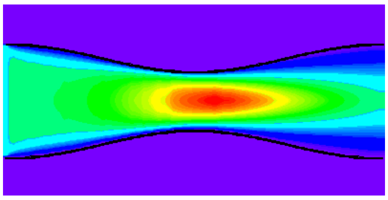

(b)

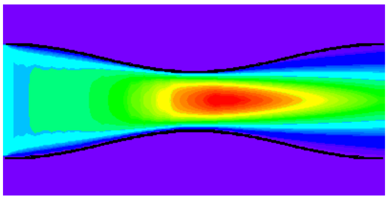

(c)

Fig. 3 Axial velocity distribution for (a) case I, (b) case II, and (c) case III

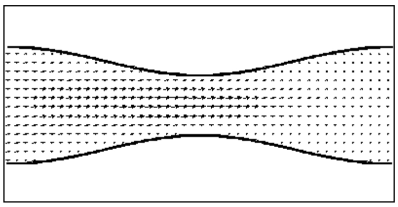

(a)

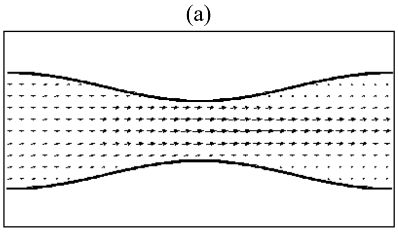

(b)

Fig. 4 Velocity vector plot for (a) case I and (b) case III

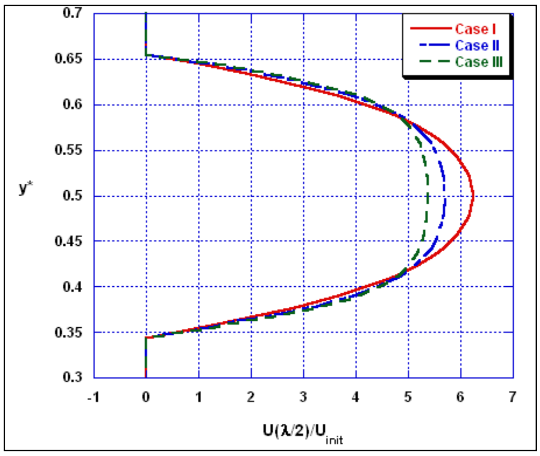


Fig. 5 Velocity profiles at the mid-section of the wave for the different cases considered

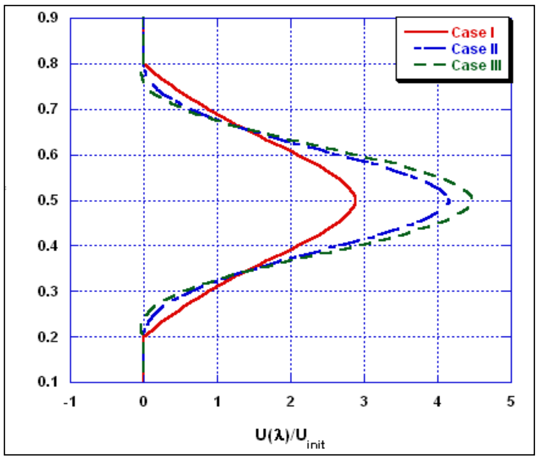


Fig. 6 Velocity profiles at the end-section of the wave for the different cases considered

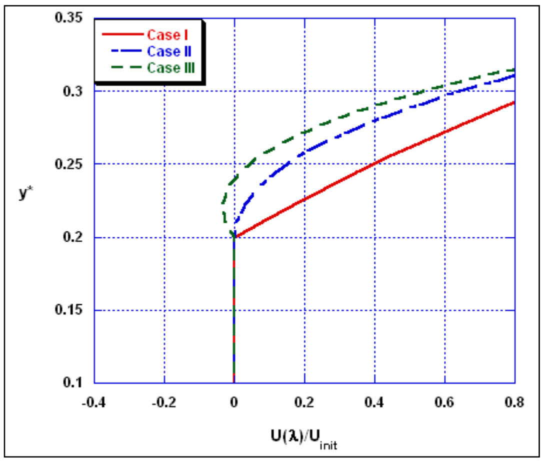


Fig. 7 The existence of flow separation at the end-section of the wave for the different cases considered

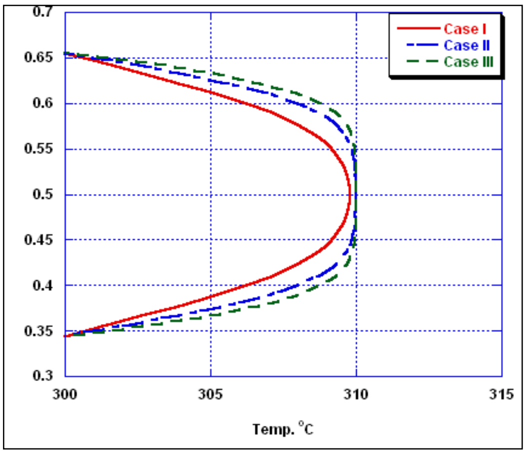


Fig. 8 Temperature profiles at the mid-section of the wave for the different cases considered

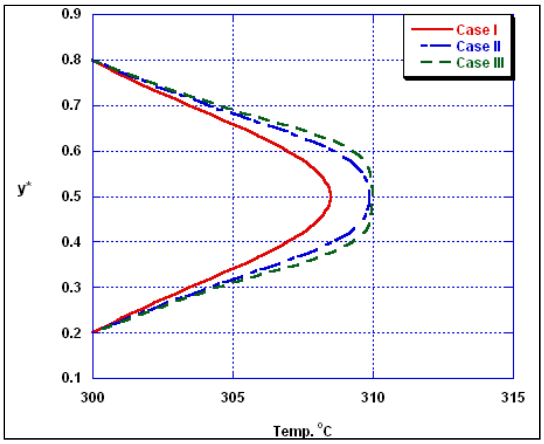


Fig. 9 Temperature profiles at the end-section of the wave for the different cases considered

## IV. Conclusion

Numerical simulation of fluid behavior in wavy microchannel used in microelectronic devices is investigated in this study. Effects of Reynolds number on the velocity and thermal behaviors are investigated. Three cases of Reynolds number (580, 1244, and 1910) are adopted in this study.

It is found that the separation zone begin appears when Reynolds number is greater than 1910 at the end-section of the wave. Also it is found that there is a contradiction in the dimensionless maximum velocity at the mid and the end section of the wave with increasing Reynolds number. The maximum temperature at the center line of the microchannel at the mid-section increases as Reynolds number increases until it reaches the flat behavior (turbulent behavior) when Reynolds number is equal or greater than 1244.

## References

[1] I. Hassan, P. Phutthavong, M. Abdelgawad, Microchannel heat sinks: an over view of the state-of-the-art, Microscale Therm. Eng. 8 (2004) 183–205.

[2] D.B. Tuckerman, R.F.W. Pease, High-performance heat-sinking for VLSI, IEEE, Electr. Dev. L. 2 (5) (1981) 126–129.

[3] M.K. Kang, J.H. Shin, H.H. Lee, K. Chun, Analysis of laminar convective heat transfer in micro heat exchanger for stacked multi-chip module, Microsyst. Technol. 11 (2005) 1176–1186.

[4] S.G. Kandlikar, W.J. Grande, Evaluation of single phase flow in microchannels for high heat flux chip cooling – thermohydraulic performance enhancement and fabrication technology, Heat Transfer Eng. 25 (8) (2004) 5–16.

[5] P.S. Lee, S.V. Garimella, D. Liu, Experimental investigation of heat transfer in microchannels, Int. J. Heat Mass Transfer 48 (2005) 1688–1704.

[6] S.V. Garimella, C.B. Sobhan, Transport in microchannels – a critical review, Annu. Rev. Heat Transfer 13 (2003) 1–50.

[7] P.S. Lee, S.V. Garimella, Thermally developing flow and heat transfer in rectangular microchannels of different aspect ratios, Int. J. Heat Mass Transfer 49 (2006) 3060–3067.

[8] N.R. Rosaguti, D.F. Fletcher, B.S. Haynes, Laminar flow and heat transfer in a periodic serpentine channel with semi-circular crosssection, Int. J. Heat Mass Transfer 49 (17-18) (2006) 2912–2923.

[9] N.R. Rosaguti, D.F. Fletcher, B.S. Haynes, Laminar flow and heat transfer in a periodic serpentine channel, Chem. Eng. Technol. 28 (3) (2005) 353–361.

[10] P.E. Geyer, N.R. Rosaguti, D.F. Fletcher, B.S. Haynes, Laminar flow and heat transfer in periodic serpentine mini-channels, J. Enhanced Heat Transfer 13 (4) (2006) 309–320.

[11] P.E. Geyer, N.R. Rosaguti, D.F. Fletcher, B.S. Haynes, Laminar thermohydraulics of square ducts following a serpentine channel path, Microfluid. Nanofluid. 2 (3) (2006) 195–204.

[12] P.E. Geyer, D.F. Fletcher, B.S. Haynes, Laminar flow and heat transfer in a periodic trapezoidal channel with semi-circular crosssection, Int. J. Heat Mass Transfer 50 (17–18) (2006) 3471–3480.

[13] R.M. Manglik, J. Zhang, A. Muley, Low Reynolds number forced convection in three-dimensional wavy-plate-fin compact channels: fin density effects, Int. J. Heat Mass Transfer 48 (8) (2005) 1439–1449.

[14] H.M. Metwally, R.M. Manglik, Enhanced heat transfer due to curvatureinduced lateral vortices in laminar flows in sinusoidal corrugated-plate channels, Int. J. Heat Mass Transfer 47 (10–11) (2004) 2282–2292.

[15] A. F. Khadrawi, A. Othman and M. A. Al-Nimr, Transient free convection fluid flow in a vertical microchannel as described by the hyperbolic heat conduction model, Int. J. Thermophysics, Vol. 26, pp.905, 2005.

[16] M. A. Al-Nimr, and A. F. Khadrawi, Thermal behavior of a stagnant gas convicted in a horizontal microchannel as described by the dual-phase-lag heat conduction model, Int. J. Thermophysics, Vol. 25, pp. 1953, 2004.

[17] J. Al-Jarrah, A. F. Khadrawi, and M. A. Al-Nimr, Film condensation on a vertical micro-channel, Int. Communication in Heat and Mass Transfer, Vol. 35(9), pp. 1172-1176, 2008.

[18] A. F. Khadrawi and Ahmad Al-Shyyab, Slip Flow and Heat Transfer in Axially Moving Micro-Concentric cylinders, International Communications in Heat and Mass Transfer, 37, 8, pp.1149–1152, 2010.

[19] M. A., Al-Nimr, A. M., Maqapleh, A. F. Khadrawi, and Ammourah S. A.: “Fully developed thermal behaviors for parallel flow microchannel heat exchanger”, International Communications in Heat and Mass Transfer Vol. 36, pp 385–390, 2009.

[20] M. Maqableh, A. F. Khadrawi, M. A. Al-Nimr, S. A. Ammourah and A. C. Benim, "Heat Transfer Characteristics of Parallel and Counter Flow Microchannel Heat Exchangers with Varying Wall Resistance" Progress in Computational Fluid Dynamics, 11(5), pp. 318-328, 2013.

[21] Patankar, SV. Numerical Heat Transfer and Fluid Flow. Hemisphere Publishing Corporation 1980.

[22] Balabel A. Numerical simulation of two-dimensional binary droplets collision outcomes using the level set method, International Journal of Computational Fluid Dynamics 2012;26(1): 1-21.

[23] Balabel A. Numerical Prediction of Turbulent Thermocapillary Convection in superposed Fluid Layers with a free Interface, International Journal of Heat and Fluid Flow 2011;32(6): 1226-1239.

[24] Balabel A. A New Numerical Method for Simulating Two-Fluid Interfacial Flow using Level Set Method, International Journal of Control, Automation and Systems 2013;.2(3): 31-40.

[25] Balabel A Numerical Modelling of Turbulence Effects on Droplet Collision Dynamics using the Level Set Method. Computer Modeling in Engineering and Sciences (CMES) 2012; 89(4):283-301.